THEORETICAL MODELING OF A CAVITATING MOONEY-RIVLIN MICROSHELL, WITH MULTIPLE SCALE ANALYSIS

Naude J.* Méndez F., Yepes C. and Navarrete M.
*Author for correspondence
Departamento de Termofluidos, Facultad de Ingenieria
Universidad Nacional Autonoma de México
Ciudad Universitaria, Coyoacán
México D. F.
E-mail: jorge_naude@comunidad.unam.mx

ABSTRACT

In this paper we propose a mathematical model with tensorial analysis for a single cavitating microshell bubble immersed in a newtonian liquid, excited by an ultrasound field. We obtain a system of nonlinear differential equations Rayleigh-Plesset kind for a thin shell working as a Mooney Rivlin hyperelastic solid. Numerical solutions of the full equation are obtained, for periodic and nonperiodic oscillations, for different values of the elastic parameters. We also present a frequency analysis for the nonlinear behaviour of the system by obtaining an analytical solution with the method of Multiple Scale Analysis. All of these is carried out taking into account the values of the parameters used in the Contrast Agents phenomena.

INTRODUCTION

Contrast agents used on ultrasound diagnosis, drug delivery and perforation are hollow microspheres. These can be modelled as microbubbles immersed in an infinite liquid with a gas inside, insonified by an oscillating high frequency pressure field. In recent years works are dedicated to the modelling and prediction of its behaviour [1-5]. Perhaps the attempts of measurements of their mechanical properties [6], it's difficult to identify the real nature of the substance that forms the agent [7]. Therefore we propose to consider it as a hyperelastic thin shell solid following the approximation [5], this mean,s if the shell thickness is small compared to the radius of the the bubble the whole deformation can be represented by the outside radius deformations.

In the present work we propose a mathematical model for the shell as a hyperelastic Mooney-Rivlin solid using the Rayleigh-Plesset equation. Also we give numerical solution for the time versus radius with the phase space, together with an analytical solution for the damping parameters using multiple scale perturbation analysis.

NOMENCLATURE

a	[-]	Non dimensional outside radius
a^*	[-]	Real part in perturbation analysis
A	[-]	Constant for the solution proposed
p_l	[N/m]	Liquid pressure
p_A	[N/m]	Driving pressure
p_{g0}	[N/m]	Initial gas pressure inside the bubble
P_A	[-]	Non dimensional driving pressure
R	[m]	Bubble radius
r	[m]	Radial coordinate
Re	[-]	Reynolds Number
St	[-]	Strouhal Number
t	[s]	time
t_c	[s]	Characteristic time
T_n	[-]	Time scales
u	[-]	Perturbation variable
u'	[m]	deformation
w_1 w_2	[N/m^2]	Mooney-Rivlin Elastic first and second constants
x	[-]	relative amplitude in perturbation analysis

Special characters

α	[-]	Non dimensional Mooney-Rivlin first constant
β	[-]	Non dimensional Mooney-Rivlin second constant
α^* β^*	[-]	Non dimensional Mooney-Rivlin first and second perturbation scaled constants
σ	[-]	Detuning parameter
σ_{rr}	[N/m^2]	Radial stress component
$\sigma_{\theta\theta}$	[N/m2]	Angular stress component
ε	[-]	Ratio between the difference of inside and outside initial radiuses and the initial radius of the bubble
λ	[-]	Densities ratio
ρ_s	[kg/m^3]	Solid density
ρ	[kg/m3]	Liquid density
γ	[-]	Adiabatic index
ξ	[-]	Time Scaling parameter
ω_0	[-]	Dimensionless natural frequency
μ_l	[Pas]	Liquid viscosity
η	[-]	Detune time for the solution

Subscripts

10	Inside initial
20	Outside initial
go	Initial equilibrium

MATHEMATICAL MODEL

In the first place, for the solid shell deformations we have the Cauchy´s stress equation for a spherical nonstationary symmetrical solid

$$\frac{\partial \sigma_{rr}}{\partial r}+\frac{2\left(\sigma_{rr}-\sigma_{\theta\theta}\right)}{r}=\rho_s\frac{\partial^2 u`}{\partial t^2} \qquad (1)$$

For the spherical deformation u´ can be written

$$u`=r-R \qquad (2)$$

The difference of the radial coordinate minus the shell radius, and writing the stress for the spherical Mooney-Rivlin stress model

$$\sigma_{rr}-\sigma_{\theta\theta}=2w_1\left(\frac{R^4}{r^4}-\frac{r^2}{R^2}\right)+2w_2\left(\frac{R^2}{r^2}-\frac{r^4}{R^4}\right) \quad (3)$$

With (2), substituting (3) on (1) and integrating from the inside radius R_1 to the outside radius R_2 as in [8] we get a differential equation for the difference between the outside and inside stresses of the shell

$$\sigma_{rr}\left(r=R_2\right)-\sigma_{rr}\left(r=R_1\right)=$$
$$\rho_s\left(-R_2\frac{d^2R_2}{dt^2}\left(1-\frac{R_2}{R_1}\right)+\left(\frac{dR_2}{dt}\right)^2\left[-\frac{3}{2}+2\frac{R_2}{R_1}-\frac{1}{2}\left(\frac{R_2}{R_1}\right)^4\right]\right)$$
$$+w_1\left(\frac{R_{20}{}^4}{R_2{}^4}-\frac{R_{10}{}^4}{R_1{}^4}+4\frac{R_{20}}{R_2}-4\frac{R_{10}}{R_1}\right)+$$
$$w_2\left(2\frac{R_{20}{}^2}{R_2{}^2}-2\frac{R_{10}{}^2}{R_1{}^2}+4\frac{R_2}{R_{20}}-4\frac{R_1}{R_{10}}\right) \quad (4)$$

The Rayleigh-Plesset equation for a single bubble immersed in a liquid, in this case it is assumed valid from the surface of the bubble R_2 to infinite along the radial direction

$$\rho_l\left[\frac{d^2R_2}{dt^2}+\frac{3}{2}\left(\frac{dR_2}{dt}\right)^2\right]=p_l\left(R_2\right)-p_\infty \quad (5)$$

Equations (4) and (5), must be coupled, in (4) we have the shell motions, in (5) we have the liquid motions surrounding the shell. The coupling comes from a balance of stresses of both substances. On the outer surface we have the balance of stresses, one the radial stress of the solid and on the other side the pressure and the viscous stress in the liquid such as

$$p_l\left(R_2\right)+4\frac{\mu}{R_2}\frac{dR_2}{dt}=-\sigma_{rr}\left(r=R_2\right) \quad (6)$$

On the inside we have the bubble filled with gas that obeys the adiabatic ideal gas law for compression. For this case the solid stress at the inner surface balances with the pressure of the gas.

$$\sigma_{rr}\left(r=R_1\right)=-p_{g0}\left(\frac{R_1}{r_1}\right)^{3\gamma} \quad (7)$$

On substituting (7) and (6) in (4) and adding it to (5) we get an equation for the shell on the outside surrounded by a liquid and on the inside filled with an adiabatic ideal gas. Eq. (8) is a general modified Rayleigh-Plesset equation including the Mooney-Rivlin hyperelastic model.

In the first two terms in the left we find the ratio of densities λ, for all values different from zero both shell and liquid move simultaneously, being these the inertial effects. The third term is the Newtonian viscous effect. On the right hand we find the pressure inside the bubble, the pressure in the bulk liquid and the stresses generated from the hyperelastic deformation, from the inside and outside surfaces of the bubble.

$$R_2\frac{d^2R_2}{dt^2}\left[1-\lambda\left(1-\frac{R_2}{R_1}\right)\right]+$$
$$\left(\frac{dR_2}{dt}\right)^2\left[\frac{3}{2}-\lambda\left(\frac{3}{2}-2\frac{R_2}{R_1}+\frac{1}{2}\left(\frac{R_2}{R_1}\right)^4\right)\right]+$$
$$4\frac{\mu}{\rho R_2}\frac{dR_2}{dt}=\frac{p_{g0}}{\rho}\left(\frac{R_1}{r_1}\right)^{3\gamma}-\frac{p_\infty}{\rho}-$$
$$w_1\left(\frac{R_{20}{}^4}{R_2{}^4}-\frac{R_{10}{}^4}{R_1{}^4}+4\frac{R_{20}}{R_2}-4\frac{R_{10}}{R_1}\right)-$$
$$w_2\left(2\frac{R_{20}{}^2}{R_2{}^2}-2\frac{R_{10}{}^2}{R_1{}^2}+4\frac{R_2}{R_{20}}-4\frac{R_1}{R_{10}}\right) \quad (8)$$

This equation can be simplified with the thin layer approximation [5] with the aid of

$$R_1=R_2\left[1-\left(\frac{3\varepsilon}{\left(1+\varepsilon\right)}\right)^3\frac{R_{20}^3}{R^3{}_2}\right]^{\frac{1}{3}} \quad (9)$$

Where

$$\frac{R_{20}-R_{10}}{R_{10}}=\varepsilon \quad (10)$$

When $\varepsilon\rightarrow 0$ the thin shell approximation is reached and for $\varepsilon=0$; we recover the original R-P equation.

In order to obtain the control parameters we introduce the following nondimensional variables

$$a=\frac{R_2}{R_{20}};\tau=\frac{t}{t_c}$$

And taking into account

$$t_c=\left(\frac{\rho_l R_{20}}{p_{go}}\right)^{1/2}$$

$$\alpha=\frac{w_1t_c^2}{\rho R_{20}{}^2};\beta=\frac{w_2t_c^2}{\rho R_{20}{}^2};P_A=\frac{p_A}{p_{g0}};St=\omega t_c$$

$$\mathrm{Re}=\frac{\sqrt{\rho_l p_{g0}R_{20}^2}}{\mu_l}$$

Eq. (8) can be rewritten as

$$
a\ddot{a}\left[1-\lambda\left(1-\left[1-\left(\frac{3\varepsilon}{(1+\varepsilon)}\right)^{3}a^{3}\right]^{-\left(\frac{1}{3}\right)}\right)\right]+
$$
$$
\dot{a}^{2}\left[\frac{3}{2}-\lambda\left(\begin{array}{l}\frac{3}{2}-2\left[1-\left(\frac{3\varepsilon}{(1+\varepsilon)}\right)^{3}a^{3}\right]^{-\left(\frac{1}{3}\right)}\\ +\frac{1}{2}\left[1-\left(\frac{3\varepsilon}{(1+\varepsilon)}\right)^{3}a^{3}\right]^{-\left(\frac{4}{3}\right)}\end{array}\right)\right]
$$
$$
+\frac{4}{\mathrm{Re}}\frac{\dot{a}}{a}=\left(\frac{1}{a}\right)^{3\gamma}(1+\varepsilon)^{-3\gamma}\left[1-\left(\frac{3\varepsilon}{(1+\varepsilon)}\right)^{3}a^{3}\right]^{-\gamma}
$$
$$
+-1-P_{A}\cos\left(St\tau\right)-
$$
$$
-\alpha\left(\begin{array}{l}\left(\frac{1}{a}\right)^{4}-\left(\frac{1}{a}\right)^{4}(1+\varepsilon)^{-4}\left[1-\left(\frac{3\varepsilon}{(1+\varepsilon)}\right)^{3}a^{3}\right]^{-\left(\frac{4}{3}\right)}\\ +4\left(\frac{1}{a}\right)\ -4\left(\frac{1}{a}\right)(1+\varepsilon)^{-1}\left[1-\left(\frac{3\varepsilon}{(1+\varepsilon)}\right)^{3}a^{3}\right]^{-\left(\frac{1}{3}\right)}\end{array}\right)-
$$
$$
2\beta\left(\begin{array}{l}\left(\frac{1}{a}\right)^{2}-\left(\frac{1}{a}\right)^{2}(1+\varepsilon)^{-2}\left[1-\left(\frac{3\varepsilon}{(1+\varepsilon)}\right)^{3}a^{3}\right]^{-\left(\frac{2}{3}\right)}\\ -2a+2a(1+\varepsilon)^{-1}\left[1-\left(\frac{3\varepsilon}{(1+\varepsilon)}\right)^{3}a^{3}\right]^{-\left(\frac{1}{3}\right)}\end{array}\right)
$$

(11)

This last equation is written for the outside radius only, but the influence of the inner radius is present through the parameter ε. In order to validate the thin layer approximation; this equation should be linearized around this parameter to give

$$
a\ddot{a}\left[1+\frac{\lambda\varepsilon}{a^{3}}\right]+\frac{3}{2}\dot{a}^{2}+\frac{4}{\mathrm{Re}}\frac{\dot{a}}{a}=
$$
$$
\left(\frac{1-3\gamma\varepsilon}{a^{3\gamma}}\right)\left(1+\frac{3\gamma\varepsilon}{a^{3}}\right)-1-P_{A}\cos\left(St\tau\right)
$$
$$
-\frac{\alpha}{a^{4}}\left(1-\left(1-4\varepsilon\right)\left(1+\frac{4\varepsilon}{a^{3}}\right)+4a^{3}\left[1-\left(1-\varepsilon\right)\left(1+\frac{\varepsilon}{a^{3}}\right)\right]\right)-
$$
$$
-2\frac{\beta}{a^{2}}\left(1-\left(1-2\varepsilon\right)\left(1+\frac{2\varepsilon}{a^{2}}\right)-2a^{3}\left[1-\left(1+\varepsilon\right)\left(1-\frac{\varepsilon}{a^{3}}\right)\right]\right)
$$

(12)

Equation (12) shows that for the second term in the left side, terms associated with λ are lost, cancelled algebraically, some information regarding the inside radius is somehow obscured.

Linearizing again with respect to ε, eliminating terms of O(ε^2) and making the product λε tend to zero the final equation is

$$
a\ddot{a}+\frac{3}{2}\dot{a}^{2}+\frac{4}{\mathrm{Re}}\frac{\dot{a}}{a}=\left(\frac{1}{a^{3\gamma}}\right)-\frac{4\alpha\varepsilon}{a^{4}}\left(a^{3}-\frac{1}{a^{3}}\right)-\frac{4\beta\varepsilon}{a^{2}}\left(a^{3}-\frac{1}{a^{3}}\right)-
$$
$$
1-P_{A}\cos\left(St\tau\right)
$$

(13)

The relevance of (13) is that the elastic parameters are scaled by ε the thin shell parameter, giving a balance of terms for the whole equation.

To close the model the initial conditions are

$$
a(0)=1 \qquad (14)
$$
$$
\dot{a}(0)=0
$$

PERTURBATION ANALYSIS

There are many works that had used a perturbation analysis for the R-P equation, to get equations for small amplitude driving pressure and small oscillations around the equilibrium radius [2,9-10]. The objective of the present analysis is to get the natural frequency for the primary resonances and a steady state solution for the frequency dependent amplitude response for the shell. In this case the multiple physical events that a nonlinear oscillation can exhibit for different times, suggests that a multiple scale analysis is suitable for this. Formally speaking, "only methods that yield a nonuniform expansion can be used for nonlinear oscillations" [11].

Expanding the equilibrium radius in terms of a relative amplitude x

$$
a=1+\xi x \qquad (15)
$$

Where ξ is a small parameter, taking (15) to (13) and expanding in powers of x up to the third order (cubic terms)

$$
\ddot{x}+\frac{3}{2}\dot{x}^{2}\xi\left(1-\xi x+(\xi x)^{2}-(\xi x)^{3}\right)+\frac{4\dot{x}}{\mathrm{Re}}\left(1-2\xi x+3(\xi x)^{2}-4(\xi x)^{3}\right)
$$
$$
=\frac{1}{\xi}\left(1-(3\gamma+1)\xi x+\frac{1}{2}(\xi x)^{2}\left[(3\gamma+1)(3\gamma+2)\right]-\frac{(\xi x)^{3}}{3}\left[(3\gamma+1)1+\frac{3}{4}(3\gamma+1)1+\frac{17}{2}(3\gamma+1)\right]\right)+
$$
$$
\frac{1}{\xi}(\xi x)^{4}(3\gamma+1)\left(\frac{1}{4}+\frac{11}{24}(3\gamma+1)+\frac{1}{4}(3\gamma+1)^{2}+\frac{1}{24}(3\gamma+1)^{4}\right)-
$$
$$
-\frac{4\alpha^{*}}{\xi}\left(1-2\xi x+3(\xi x)^{2}-4(\xi x)^{3}\right)\left(1-\left(1-6\xi x+21(\xi x)^{2}-56(\xi x)^{3}+126(\xi x)^{4}\right)\right)-
$$
$$
\frac{4\beta^{*}}{\xi}\left(1-\left(1-6\xi x+21(\xi x)^{2}-56(\xi x)^{3}+126(\xi x)^{4}\right)\right)-
$$
$$
-\frac{1}{\xi}\left(1+p_{A}\cos\left(St\tau\right)\right)\left(1-\xi x+(\xi x)^{2}-(\xi x)^{3}\right)
$$

(16)

The MS method [11] requires that the equation should be balanced so that the damping terms, the forcing and the dissipative terms must be in the same scale order, so the variables should take the following scales

$$
p_{A}=\xi^{3}f;\,x=u;\,\frac{\xi^{2}}{\mathrm{Re}}\rightarrow 1
$$

For starting the MS method, the following expansions in time and derivatives should take the form

$$u=u_0\left(T_0,T_1,T_2\right)+\xi u_1\left(T_0,T_1,T_2\right)+\xi^2u_2^2\left(T_0,T_1,T_2\right)$$
$$T_n=\xi^n\tau;n=0,1,...$$
$$\frac{d}{d\tau}=\sum_{n=0}\xi^nD_n,D_n=\frac{\partial}{\partial T_n} \tag{17}$$

Substituting (16) in (15) and equating powers of chi

$$D_0^2u_0+\omega_0^2u_0=0 \tag{18}$$

The zeroth order with the natural frequency

$$\omega_0^2=3\gamma+24\left(\alpha^*+\beta^*\right) \tag{19}$$

First and second order

$$D_0^2u_1+\omega_0^2u_1=-2D_0D_1u_0-\frac{3}{2}\left(D_0u_0\right)^2+ u_0^2\left[\frac{9\gamma^2+9\gamma+2}{2}+132\alpha^*+64\beta^*-1\right] \tag{20}$$

$$\begin{aligned}D_0^2u_2+\omega_0^2u_2&=-2D_0D_1u_1-\left(D_1^2+2D_0D_2\right)u_0-\\&3\left(D_0u_0\right)\left(D_0u_1\right)-3\left(D_0u_0\right)\left(D_1u_0\right)+\frac{3}{2}\left(D_0u_0\right)^2u_0-4\frac{1}{\mathrm{Re}}\left(D_0u_0\right)+\\&2u_1u_0\left\{\left(3\gamma+1\right)\left(3\gamma+2\right)+\frac{1}{2}\left(264\alpha^*+168\beta^*-2\right)\right\}-\\&-u_0^3\left[\begin{matrix}\left(3\gamma+1\right)\left\{1+\frac{3}{4}\left(3\gamma+1\right)\left[1+\frac{17}{2}\left(3\gamma+1\right)\right]\right\}+\\464\alpha^*+224\beta^*+1\end{matrix}\right]+\\&f\cos\left(\omega_0T_0+\sigma T_2\right)\end{aligned} \tag{21}$$

Where the time scale can be defined as the natural frequency with a small detune

$$St=\omega_0+\xi^2\sigma$$

Proposing a complex solution derived from the homogeneous equation (17)

$$u_0=A\left(T_1,T_2\right)e^{i\omega_0T_0}+c.c. \tag{22}$$

Where $c.c$ is the complex conjugate

Substituting (22) in (20), the equation can show the secular term which is

$$-2D_1Ae^{i\omega_0T_0}=0 \tag{23}$$

In general A is function of the two time scales but (23) shows that

$$A=f\left(T_2\right)$$

For the next order the solution is proposed as

$$u_1=c_1A^2e^{2i\omega_0T_0}+c_2A\tilde{A}+c.c. \tag{24}$$

and the constants can be evaluated as

$$c_1=\frac{-1}{3\omega_0^2}\left[\frac{9\gamma^2+9\gamma+2}{2}+132\alpha^*+64\beta^*+\frac{1}{2}\right]$$
$$c_2=\frac{2}{\omega_0^2}\left[\frac{9\gamma^2+9\gamma+2}{2}+132\alpha^*+64\beta^*-\frac{5}{2}\right] \tag{25}$$

Applying to the second order equation the same criteria for obtaining the secular terms and proposing a solution for A

$$A=\frac{a\left(T_2\right)}{2}e^{i\eta\left(T_2\right)} \tag{26}$$

The secular terms equalled to zero gives one equation that can be separated into its real and imaginary parts

$$\omega_0a\frac{\partial\eta}{\partial T_2}+ \frac{1}{8}a^3\left\{\begin{matrix}3+\left(c_1+c_2\right)\left\{2\left(3\gamma+1\right)\left(3\gamma+2\right)+\left(264\alpha^*+168\beta^*-2\right)\right\}-\\-3\left[\begin{matrix}\left(3\gamma+1\right)\left\{1+\frac{3}{4}\left(3\gamma+1\right)\left[1+\frac{17}{2}\left(3\gamma+1\right)\right]\right\}+\\464\alpha^*+224\beta^*+1\end{matrix}\right]\end{matrix}\right\} +\frac{1}{2}f\cos\bar{\gamma}=0 \tag{27}$$

$$-\omega_0\frac{\partial a}{\partial T_2}-\frac{2}{\mathrm{Re}}\omega_0a+\frac{1}{2}f\sin\bar{\gamma}=0 \tag{28}$$
$$\bar{\gamma}=\sigma T_2-\eta$$

To get the steady state response the partial derivatives of the equations are set to zero and combining (28) and (27) yields

$$\frac{f^2}{4\omega_0^2}=\left(a\sigma+\frac{1}{8}a^3\left\{\begin{matrix}3+\left(c_1+c_2\right)\left\{2\left(3\gamma+1\right)\left(3\gamma+2\right)+\left(264\alpha^*+168\beta^*-2\right)\right\}-\\-3\left[\left(3\gamma+1\right)\left\{1+\frac{3}{4}\left(3\gamma+1\right)\left[1+\frac{17}{2}\left(3\gamma+1\right)\right]\right\}+464\alpha^*+224\beta^*+1\right]\end{matrix}\right\}\right)^2+ +\frac{4}{\mathrm{Re}^2}a^2 \tag{30}$$

NUMERICAL SOLUTION

Equation (13) is solved with a Runge Kutta 4th order method in INTEL Fortran. The representative values for the problem of contrast agents can be found in [5-7], for *117 <P_A <430MPa, 10<w_1<120MPa, 5<w_2<80MPa, R_{20}=4μm, γ=1.4,*

ρ_l*=1000kg/m*^{3}, ω*=3MHz*, ε*=0.05* and p_{go}*=100kPa*. These values are for water and air in liquid and gas sides and the hyperelastic constants for the solid shell.

In fig. 1 dimensionless radius versus dimensionless time, for three different pairs of hyperelastic constants, starts with an

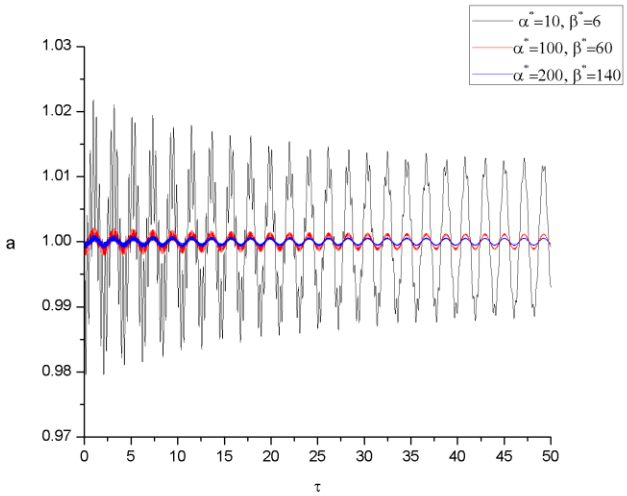

Figure 1 Radius versus time for different values of hyperelastic constants

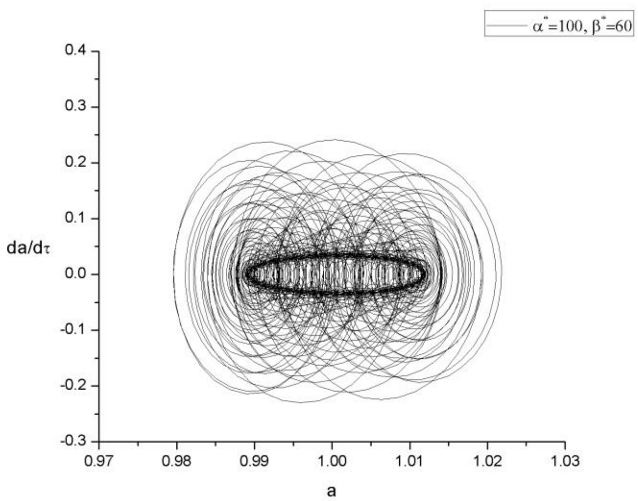

Figure 2 Phase space for α^* *=100* and β^**=60*

irregular oscillations making a transitory regime until regular oscillations are reached. This is confirmed in Fig. 2 a limit cycle appears in an ellipsoid form and suggests that this will continue until a steady mode is reached. The other cases are very similar. In fig. the influence of Reynolds Number for Reynolds 4 it shows a little transient at the beginning, stabilizing with very regular oscillations, these are smaller in amplitude compared with the 40 and 400 case, that in both cases the amplitude is almost the same and the oscillation is regular but with many harmonics. The small Reynolds is a damping and stabilizing parameter.

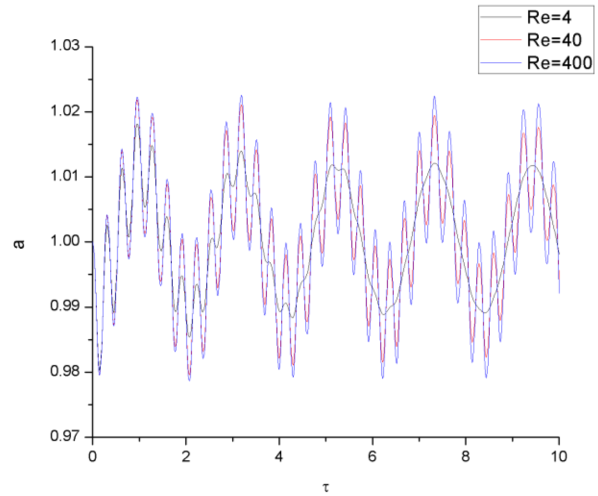

Figure 3 Radius versus time for different values of Reynolds number, α^* *=10* and β^**=6*

Figs. 4, 5 and 6 show the numerical solution for eq. 30 these are the frequency response curves. Fig. 4 shows the influence of the hyperelastic parameters. This chart seems to contradict Fig. 1, the biggest the hyperelastic parameters the smallest the spike, this seems to happen because the fast response of the material to the forcing, just in this small restricted domain of small amplitude oscillations the material responds very fast.

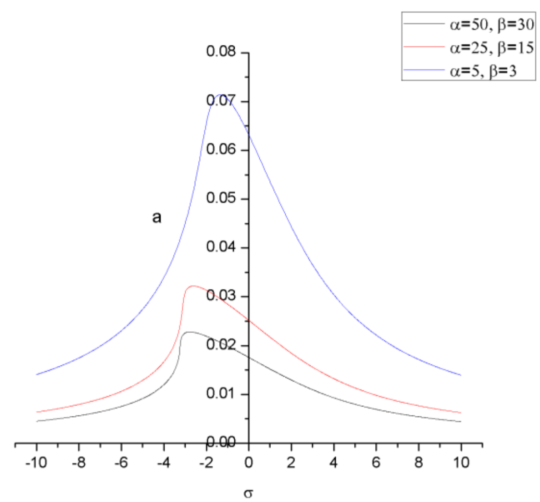

Figure 4 Frequency response curves fixating the forcing amplitude and the Reynolds number

Fig.5 shows the influence of the Reynolds number with fixated hyperelastic parameters and the same forcing amplitude, in this case the Reynolds damps the spike. For Fig. 6 it is clear the influence of the forcing parameter f, the smallest is the smallest the spike.

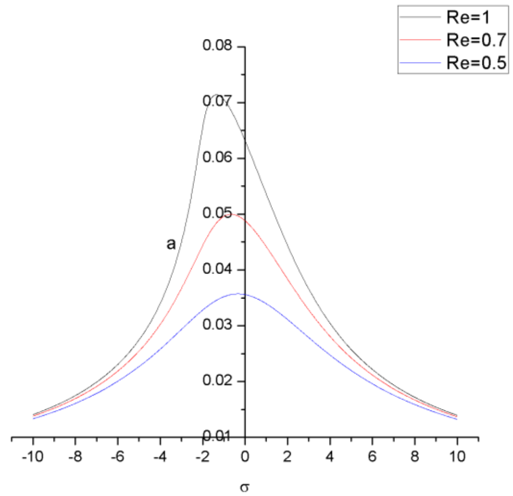

Figure 5 Frequency response curves fixating the forcing amplitude and the hyperelastic constants

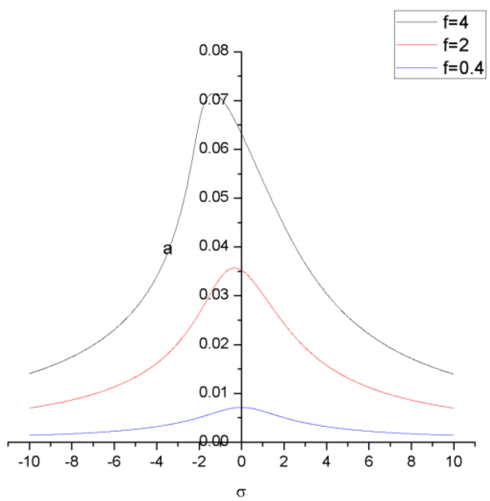

Figure 6 Frequency response curves fixating the Reynolds Number amplitude and the hyperelastic constants

TRENDS AND RESULTS

In the curves presented here the collapse was not found for the amplitudes exemplified, for higher amplitudes a sudden collapse might be found strongly dependent on the Reynolds number and not in the hyperelastic constants, in a previous work this is what happened.

For the multiple scale analysis the natural frequency and frequency response curves are clearly dependant on the hyperelastic parameters. In the process it was found that the damping influence only appeared at the third power of the expanded variable u taking the problem to the second order.

CONCLUSION

The numerical results of figs. 1-3 indicate that there is not going to be a sudden collapse on the contrary the oscillations will stabilize as the limit cycle shows, although fig. 3 shows a harmonic transient, this tends to stability. The amplitude of the oscillations are of the same order comparing with low Reynolds number and low values of the hyperelastic parameters, however with a stronger material the amplitude is significantly reduced and even with an increment of one order of magnitude in the parameters the amplitude seem to keep the same value. For sure it is needed to explore more examples in order to find the collapse.

The frequency response curves show that this model can be stable and oscillatory stable, and the tendency will be towards no resonance. The hyperelastic parameters show more damping and more deviation from the middle point compared with the Reynolds damping.

AKNOWLEDGEMENTS

This paper was financed by the Proyecto PAPIIT IN112515

REFERENCES

[1] Chetty K., Stride E., Sennoga C. A., Hajnal J. A., and Eckersley R. J., High-speed optical observations and simulation results of SonoVue microbubblesat low-pressure insonation, *I.E.E.E. Transactions on Ferroelectrics and Frequency control*, vol. 55, No. 6, June 2006.

[2] Allen J. S. and Roy R. A., Dynamics of gas bubbles in viscoelastic fluids. I. Linear viscoelasticity, *J. Acoust. Soc. Am*., vol. 107, No. 6, June 2000.

[3] Marmottant P., Van der Meer S., Emmer M., Versluis M., de Jong N., Hilghenfeldt S. and Lohse D., *A model for large amplitude oscillations of coated bubbles accounting for buckling and rupture, J. Acoust. Soc. Am.*, vol. 118, No. 8, December 2005.

[4] Church C., The effects of an elastic solid surface layer on the radial pulsations of gas bubbles, *J. Acoust. Soc. Am*., vol. 97, No. 1510 1995.

[5] Hoff L. , Acoustic characterization of contrast agents for medical ultrasound, Kulwer Academic Publishers2010.

[6] Rachik M.,Barthes-Biesel D., Carin M. and Edwards-Levy F., Identification of the elastic properties of an artificial capsule membrane, *J. of Colloid and Interface Sci.* vol. 301 2006
with the compression test: Effect of thickness

[7] de Jong N., Frinking P. J. A, Bouakaz A., Goorden M., Schourmans T., Xu J. P., and Mastik F., Optical imaging of contrast agent microbubbles in an ultrasound field with a 100-MHz camera, *Ultrasound Med. Biol*., vol. 26, 2000.

[8] Roussos N., Mason D. P., Hill D. L., On non-linear radial oscillations of an incompressible, hyperelastic spherical shell, *Mathematics and Mechanics of Solids*, vol. 7, 2002

[9] Prosperetti A., Nonlinear oscillations of gas bubbles in liquids: Steady state solutions, *J. Acoust. Soc. Am*. Vol. 56, 1974.

[10] Francescutto A. and Nabergoj R., Steady-state oscillations of gas bubbles in liquids: Explicit formulas for frequency-response curves, *J. Acoust. Soc. Am*. Vol. 731983

[11] Nayfeh A.H. and Mook D.K., Nonlinear Oscillations, Wiley, New York, 1979

[10] Dirker J, Liu W, Van Wyk, J.D., and Meyer J.P., Evaluation of embedded heat extraction for high power density integrated electromagnetic passives, *Proceedings of the 35th I.E.E.E. Power Electronics Specialist conference*, Aachen, Germany, Paper number 11430, 21-25 June, 2004.